Modeling Molecules for Field-Coupled Nanocomputing Circuit Design

Modeling Molecules for Field-Coupled Nanocomputing Circuit Design

Yuri Ardesi*‡, Federico Ravera*, Gianluca Piccinini*, Mariagrazia Graziano†
*Department of Electronics and Telecommunications, Politecnico di Torino, Torino, Italy
†Department of Applied Science and Technology, Politecnico di Torino, Torino, Italy
‡corresponding author e-mail: *yuri.ardesi@polito.it*

***Abstract*—Molecular Field-Coupled Nanocomputing (molFCN) is a highly low-power technology promising for digital electronics. It encodes information in the charge distribution of molecules and propagates it through electrostatic intermolecular interaction. Despite its potential, the molFCN technology suffers the absence of a functional design and simulation methodology. This paper provides a complete explanation of the characterization and modeling of molecules, from the molecular *ab initio* analysis to the design of molecular circuits and systems. Considering the diallyl-butane, we show how to use the ORCA package to derive, with DFT, the molecule geometry and charge distribution by correctly setting DFT functionals and basis sets. We study the molecule polarization when subjected to electric fields and enable the investigation of the interaction by exploiting the SCERPA tool. We set up the SCERPA simulation engine to simulate molecular circuits such as diallyl-butane wires. Finally, we show how to use literature results to model more complex molecules. We implement the bis-ferrocene cation in SCERPA and use it to create complex clocked logical devices. We simulate, as a means of explanation, a $0.0004\,\mu\mathrm{m}^2$ NAND gate.**

I. Introduction

MOlecular Field-Coupled Nanocomputing (molFCN) has been addressed as a highly low-power technology promising for digital electronics. The encoding of the information, following the Quantum-dot Cellular Automata paradigm [1], is based on the molecule charge distribution, and local electrostatic intermolecular interactions permit the information propagation. It presents intrinsic nanometric size and possible operations at ambient temperature [1]–[3], with calculations predicting functional behavior up to hundreds of K [2], [3]. In addition, information propagation and elaboration involve no electric current, drastically reducing the power dissipation. Notwithstanding molFCN potentially disruptive advantages, two connected problems must be solved to advance the technology. Indeed, an actual prototype has yet to be fabricated, and no effective design and simulation methodology exists [4]. Effective modeling of molFCN devices considering the real molecular physics would permit assessing the actual molFCN circuit performance and identifying the requirements of future molecules, facilitating the realization of a molecular prototype [5]. For this purpose, our group conceived a method named MoSQuiTO (MOlecular Simulator QUantum-dot cellular automata TOrino) that characterizes the molecules with Density Functional Theory (DFT) and enables circuit simulation with the Self-Consistent ElectRostatic Potential Algorithm (SCERPA). So far, the literature results regarding the characterization and the modeling of molecules are distributed on several papers, which makes it difficult for the designer to acquire all the information quickly. This paper addresses the molFCN characterization from an electronics perspective and provides a complete explanation of the characterization and modeling of molecules, from the *ab initio* analysis to the circuit and system design. We start with a brief overview of the molFCN background, highlighting its potentialities in nanoscale digital electronics and the current challenges. Then, we show how to study and model the molecule charge behavior with DFT when subjected to electric fields, enabling intermolecular interaction modeling. Integrating the molecule in the SCERPA simulator and setting up the simulation engine permits the design and simulation of circuits. This work shows the design of diallyl-butane molFCN wires. Then, to demonstrate the method generality, we show how to use literature results to model more complex molecules, such as the bis-ferrocene cation. Finally, we report the design of a 0.0004 μm^2 NAND gate.

This work provides a concrete path for analyzing, designing, and implementing future nanoscale circuits based on molFCN, which can be adapted to other emerging field-coupled nanotechnologies. This paper contributes toward realizing molFCN prototypes since it facilitates the study of cross-implication between molecular characteristics and circuit functioning, which is fundamental for fabricating molFCN circuits. The methodology aims to be general, serving as a reference for new computing paradigms based on nanoscale phenomena and enabling a physics-to-system approach, facilitating circuit and system analysis and design.

II. Background

A. Molecular Field-Coupled Nanocomputing

The molFCN technology encodes binary information in the charge distribution of molecules, implementing the Quantum-dot Cellular Automata (QCA) paradigm at the molecular scale. Several molecules have been proposed for molFCN, including diallyl-butane and bis-ferrocene, used in this work as references for modeling [6], [7]. Fig. 1(a) depicts the structure of the bis-ferrocene molecule, while Fig. 1(b) shows the binary logic encoding in a bis-ferrocene molFCN cell. The depicted cells encode logic ‘1’, ‘0’, and the NULL state. By applying an external electric field, referred to

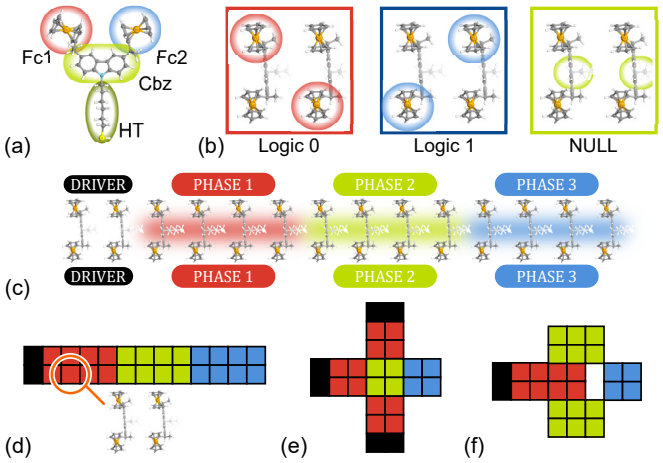

Fig. 1. Basics of molFCN: (a) bis-ferrocene molecule with highlighted functional groups, (b) molFCN cells encoding '0', '1', and NULL state, (c) wire, (d) 2-line wire, (e) 2-line majority voter, (f) 2-line inverter.

as the *clocking field*, binary information encoded in the molecular cells can be deleted by forcing molecules into the NULL state. This operation permits guided information flow in pipelined systems [8], [9]. Fig. 1(c) depicts a molFCN pipelined wire divided into three clock regions. The information propagation in molFCN is achieved through intermolecular interactions, which permits the stability of the logic encoding along the wire [10], [11]. The bistability of the information in molFCN can be linked to the geometry of the molecule, its polarizability, and the intermolecular distance [11]. In particular, it can be enhanced by strengthening the intermolecular interaction, which can be obtained by tuning the mentioned parameters or by using multiline devices, thus increasing the number of molecules [8], [11], [12]. Fig. 1(d) shows a 2-line clocked molFCN wire. The intermolecular interaction can also be used to elaborate logic information, as in the molFCN Majority Voter (MV) shown in Fig. 1(e). The MV outputs the most recurrent input logic and permits the realization of AND and OR functions by fixing one of the inputs to '0' and '1', respectively. Moreover, Fig. 1(f) shows the multiline inverter. Recent results also provided the implementation, demonstrated with physical simulation, of the planar crosswire [13], obtained by exploiting the diagonal interaction [5].

B. Modelling tools for molecular Field-Coupled Nanocomputing

The MoSQuiTo method offers researchers a robust platform for conducting device modeling from an electronics perspective. It involves molecule analysis using *ab initio* calculations, modeling with metrics like Aggregated Charge (AC) and Vin-Aggregated Charge Transcharacteristics (VACT), and circuit simulation with the SCERPA tool. Historically, the modeling of molecules in the QCA context has also been performed with the so-called Two-State Approximation (TSA), which models the molecule using quantum mechanics and offers insight into the switching behavior of bistable molecules. Recent studies, however, demonstrated that molFCN is also possible with monostable molecules [11], [14], which are better modeled by leveraging the flexibility of the MoSQuiTo method. In parallel, also QCADesigner, which is based on the TSA approach [15], is designed to simulate the general QCA paradigm and can be used to simulate molecular FCN circuits based on neutral molecules [5]. In general, the simulation of molFCN circuits with the SCERPA tool offers great flexibility regarding the molecule electrostatic nature [5]. Several tools have been developed to support diverse objectives around these methods. Specifically, MagCAD and ToPoliNano enable the simulation of molFCN technologies by integrating the SCERPA tool [12], [16], [17].

III. Simulation and Design of Molecular FCN

This section defines the MoSQuiTo methodology for analyzing, simulating, and designing molecular FCN devices and circuits. Using the diallyl-butane molecule, which has been used in several works for molFCN theoretical analysis [3], [6], [18], the section discusses: **molecule geometry optimization** for assessing molecule size and atom positions; the **calculation of equilibrium properties** to understand electrostatic characteristics of the isolated molecule; the **calculation of out-of-equilibrium properties**, thus the analysis of molecule behavior under electric fields for studying intermolecular interactions; and the **integration of the molecule into the SCERPA framework** to facilitate device and circuit simulation. Finally, this section demonstrates a functioning NAND gate using the bis-ferrocene molecule.

A. Simulation tools

This work employs several tools for the calculations. In particular, molecules are drawn with a Avogadro [19]. Alternatively, web archives such as ChemSpider[1] can be used to obtain the desired molecule structure. Avogadro is also exploited to perform preliminary molecular mechanics-based geometry optimization. The molFCN candidate molecule is then processed with DFT calculation. Specifically, the *ab initio* calculation is performed using the ORCA package [20], [21]. Figures of merit describing the molecule as an electronic device are derived from the *ab initio* calculations. Finally, the device and circuits are drawn within the MagCAD environment [16] and simulated with SCERPA [8], [12]. SCERPA iteratively solves the electrostatic interactions between the molecules forming the circuit. Since the electric modeling of the molecules originates from the *ab initio* simulations, a link is established between quantum chemical calculation and circuit level analysis [12]. SCERPA is available for free on GitHub [22].

B. Geometry optimization of the diallyl-butane molecule

To analyze the diallyl-butane molecule, we begin with its geometry. The molecule geometry must be optimized with *ab initio* precision to ensure correctness from a quantum chemistry perspective. This operation determines the position of atoms in the cartesian space by minimizing the molecule energy. The *ab initio* calculation is performed

[1]https://www.chemspider.com/

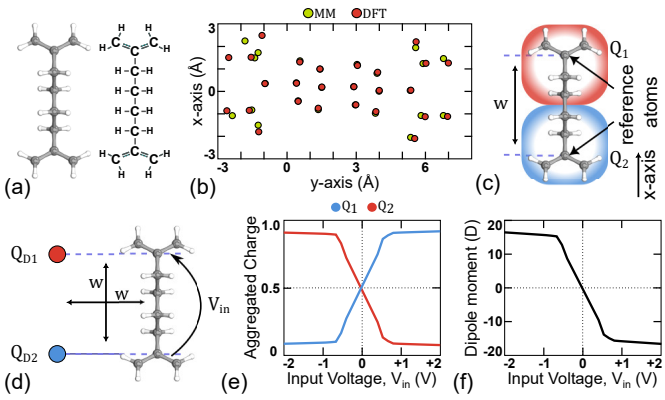

Fig. 2. Diallyl-butane cation: (a) structure of the molecule, (b) position of atoms obtained with MM and *ab initio* geometry optimization, (c) definition of the AC model, (d) interaction system, (e) VACT, (f) dipole moment variation with V_{in}.

using the ORCA package. The function associating atom positions with molecule energy is known as the Potential Energy Surface (PES), thus the optimization evaluates the PES minimum. We draw the dially-butane in this work, shown in Fig. 2(a), using Avogadro. *Ab initio* calculation is computationally expensive. Therefore, we preliminarily optimize the molecule with Molecular Mechanics (MM), which lasts a few seconds, by employing UFF force fields and the Steepest Descent algorithm. Fig. 2(b) depicts the MM optimized geometry (green dots). This operation permits evaluating a first geometry, possibly close to the PES minimum, eventually speeding up the *ab initio* calculation. The setup of the *ab initio* geometry optimization significantly impacts the accuracy of the molecule characterization. For the diallyl-butane, [1] initially proposed the Unrestricted Hartree-Fock method with STO-3G basis. However, recent studies point out that the molecule is geometrically symmetric, and the dipole moment at the thermal equilibrium should be null, which is in contrast to preliminary results obtained with STO-3G [1], [14]. The correct geometry of the diallyl-butane cation can be achieved using the Unrestricted Kohn-Sham method with CAM-B3LYP/def2-TZVP [14], [23], [24]. Additionally, employing D3 correction enhances calculation precision, particularly for electrostatic properties [25], [26].

Fig. 2(b) shows the obtained optimized geometry. The geometry, computed on six cores in 3 hours 47 minutes and 33 seconds on a GNU/Linux machine with a 32-core Intel Xeon Processor 2.3 GHz, 128 GB RAM, does not differ much from the initial geometry obtained with Avogadro, with a maximum distance of 0.1451 nm. However, given the strong dependence of the electrostatic properties on the geometries, the results would be wrong if the geometry optimization is not precisely performed. In addition, *ab initio* precision offers an accurate assessment also regarding the cationic nature of the molecule, ignored in MM simulations.

C. Single-point calculation of the diallyl-butane molecule

The geometry obtained with DFT precision in Section III-B is the basis for the subsequent single-point calculation to assess the molecule charge distribution at the thermal equilibrium. Fig. 2(c) shows the chosen reference atoms, constituting a two-charge system model for the molecule. These atoms act as the center of diallyl-butane aggregated charges (AC). For the single-point calculation, it is essential to keep consistency in computational methods, i.e. DFT functional and basis sets. To assess the molecule electrostatic characteristics, we derive the atomic charges obtained by fitting the electrostatic potential, i.e., the $CHELPG$ method [27], which have been demonstrated to effectively resemble the molecular electrostatic behavior for molFCN modeling [6]. The calculation returns an almost negligible dipole moment, μ=(0.04910 0.00127 -0.00154) a.u., confirming the consistency with the theoretical symmetry of the molecule geometry. By denoting as R_1 and R_2 the identified AC centers, we find their distance w (i.e. the molecular width) as $w = |R_1 - R_2| = 0.634420$ nm. The two aggregated charges are evaluated as follows:

$$Q_1 = \sum_{i \in G_1} Q_i \qquad Q_2 = \sum_{i \in G_2} Q_i \tag{1}$$

Q_i denotes the charge of a generic atom i, while G_1 and G_2 are the two groups of atoms contributing to the aggregated charges, as Fig.2(c) reports. The resulting ACs ($Q_1 = 0.505278$ and $Q_2 = 0.494726$) are almost identical, aligning with the observed null dipole moment.

D. Application of electric fields in the diallyl-butane molecule

In Section III-C, we determined the dipole moment of diallyl-butane at thermal equilibrium. This section investigates how the molecule charge distribution responds to electric fields to evaluate and model the intermolecular interaction. We examine the molecule in the presence of a driver molecule, emulated with two point charges, Q_{D1} and Q_{D2}, located at positions R_{D1} and R_{D2}, respectively. The driver induces an electrostatic potential, which can be calculated at any generic point R as:

$$V(r) = \frac{1}{4\pi\varepsilon_0}\left(\frac{Q_{D1}}{|R_{D1} - r|} + \frac{Q_{D2}}{|R_{D2} - r|}\right)$$

In particular, the input voltage V_{in} is evaluated as

$$V_{in} = V(R_1) - V(R_2) \tag{2}$$

In this work, we vary the driver charges Q_{D1} and Q_{D2} to examine the molecule charge distribution under various V_{in}, mimicking differently polarized molecules. Specifically, Q_{D1} ranges from -1 a.u. to 2 a.u., with 0.1 a.u. steps, whereas Q_{D2} is determined by ensuring $Q_{D1} + Q_{D2} = 1$, thus fixing the molecule cationic nature. Alternative configurations are also accepted. For instance, by fixing $Q_{D1}+Q_{D2} = 0$, we emulate the case involving neutral molecules and low transverse electric fields. The characterization typically involves input and point charges files, whose generation is streamlined by an automation bash file. The *input file* provides the input for individual ORCA calculations. Similarly, the point charges

file template contains the driver charges necessary for each ORCA calculation. The *automation file* manages the calculation by generating the N ORCA input and point charge files, providing the correct driver charges, and launching calculations. Postprocessing of output files enables the extraction of the VACT. Specifically, we compute the input voltage for each calculation using (2) and the AC using (1). Fig. 2(e) depicts the obtained VACT on $N = 31$ input voltages, which demonstrates the switching phenomenon: Q_1 is populated for positive voltage, while Q_2 is populated for negative voltage. An essential parameter for molFCN circuit design is the molecule polarizability (α), which can be derived from the dipole moment accurately calculated using the atomic charges (q_i) as:

$$\mu = \sum_i q_i r_i \tag{3}$$

r_i is the position of atomic charge q_i. Fig. 2(f) shows the obtained dipole moment as a function of V_{in}. The diallyl-butane cation polarizability, determined by differentiating the dipole moment to the electric field, evaluated approximately as $E \approx V_{in}/w$ for small E values, is α =2940.57 a.u, aligned with findings in [24]. For molecular device design, α will be used in Sec. III-E.

E. SCERPA modeling of the diallyl-butane molecule

Leveraging the modeling in Sec. III-D, we integrate the diallyl-butane cation into the SCERPA algorithm and simulate devices, e.g. a wire. The molecule geometry and electrostatic behavior must be provided for device-level simulation with the SCERPA tool. This section defines the main operative steps to perform with SCERPA, from the geometry and VACT definition to the analysis of the results.

1) Geometry definition: The SCERPA version (v4.0.1) represents all molecules with four charges. Since the modeled cation has two ACs, two ghost atoms will be added to have four charges. To insert the molecule geometry, we create a specific file divided into three sections: the **CHARGES section** defines the molecule geometry; the **ASSOCIATION section** identifies the connection among ACs for the SCERPA viewer; the **CLOCKDATA section** specifies files containing VACTs for different clock values. Notice that no clock has been considered so far. SCERPA requires at least two different clock values. Thus, two identical files have been inserted with two different clocks set at -2 V/nm and +2 V/nm. The clock values can be chosen arbitrarily, but consistent values must be used during simulation.

2) VACT definition: As mentioned, two identical files will be inserted for the VACT. The VACT file comprises 31 lines, one for each calculation N conducted in Sec. III-D. Each line denotes the cation ACs at a specific input voltage.

```
Vin[1] Q1 Q2 Q3 Q4
...
Vin[31] Q1 Q2 Q3 Q4
```

Each line requires four charges. $Q1$ and $Q2$ represent the ACs of the molecule. $Q3$ is fixed at -1 a.u., acting as a counterion to mitigate crosstalk effects, balancing the cationic nature of the molecule with a negative charge. The counterion is essential for enabling 2D circuits [5], [8]. This work uses the diallyl-butane cation only for simulating wires. Thus, as demonstrated in [8], the added charge does not impact the final results. Finally, $Q4$ is fixed at zero, irrelevant for modeling the diallyl-butane cation.

3) Simulation of a diallyl-butane wire: Once the molecule is inserted into the SCERPA framework, testing devices such as molecular wires is possible. In this context, evaluating the intermolecular distance that can be used for the wire is essential. To do this, we follow the bistability theory [11] to determine the maximum intermolecular distance (d) by inverting equation 4. The bistability factor $BF10C$ is fixed to the maximum, i.e. to 1, whereas α and w are set to 2940.57 a.u. and 0.644420 nm, according to the previous results. As a result, a maximum intermolecular distance d_{max} of 0.80788 nm is predicted to provide stable information propagation along a 10-molecule long diallyl-butane wire. Notice that BF10C is evaluated at the center of a wire, thus calculated as 2×BFN reported in [24], referred to the ending configuration.

$$BF10C = \sum_{i=1}^{10} \frac{\alpha(-1)^{i+1}}{\pi\varepsilon_0 w^2} \left(\frac{1}{i \cdot d} - \frac{1}{\sqrt{(1 \cdot d)^2 + w^2}} \right) \tag{4}$$

Fig. 3(a) reports the wire adopted in the simulation, where the first two molecules implement the input driver. Notice that we test two intermolecular distances: 0.70 nm and 0.85 nm. For the two simulations, we simulate the propagation of logic '0' with subsequent logic '1'. Given the two-dot nature of the diallyl-butane cation, no clock is applied to the wire. Fig. 3(a) shows the propagation for 0.70 nm, where white spots identify the presence of positive charges evaluated 1 $\mathring{A}$ above the Q_1 and Q_2 plane. Logic '1' correctly propagates since the distance is lower than the maximum allowed distance. A small border effect can be seen in the final molecule due to the absence of a circuit connected to the wire output. When the driver configuration is reversed, the wire retains the previous information, thus demonstrating the bistability impact in molFCN. Consequently, the propagation of new information requires a clock field, which is not implemented for this molecule. Fig. 3(b) shows the propagation for d = 0.85 nm. In this case, the distance is larger than the maximum allowed, and neither logic '0' nor '1' can propagate because of the low electrostatic interactions.

Overall, this section demonstrates the possibility of simulating molecular wires by considering molecule physics and shows the importance of the bistability theory in the design of molecular devices.

F. The bis-ferrocene molecule

The results in the previous section highlight that circuit design requires the clocking system so that the information can be canceled to permit data pipelining. For this purpose, Fig.1(a) previously showed a more complex molecule. The shown bis-ferrocene has two active dots (Ferrocenes Fc1 and Fc2), which are used to encode logic information and exploit the third dot (composed by the carbazole Cbz and

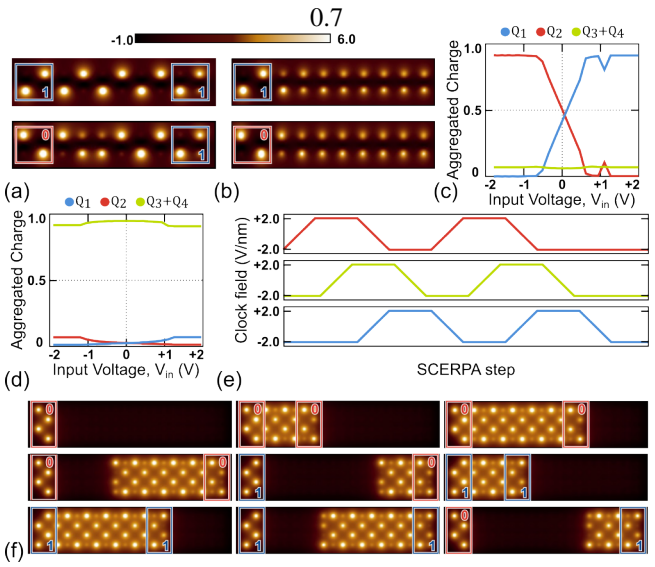

Fig. 3. (a) Information propagation results for a diallyl-butane molecular wire with intermolecular distance d = 0.70 nm. Logic '1' correctly propagates. The molecules retain the previous information, preventing information pipelining. (b) Diallyl-butane wire characterized by intermolecular distance d = 0.85 nm. The information does not propagate. (c) VACT of bis-ferrocene cation when an enhancing clocking field is applied. (d) VACT of the bis-ferrocene cation when an inhibiting clocking field is applied. (e) Clocking synchronous signal representation. (f) Information propagation along the 2-line bis-ferrocene wire. Both logic '0' and '1' correctly propagate, demonstrating the chosen clocking signals effectiveness.

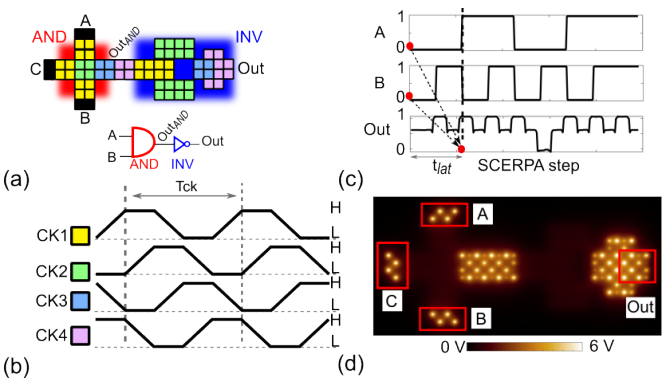

Fig. 4. (a) NAND circuit schematic and clock regions. (b) Clock signals. (c) Circuit performance analysis. The A and B inputs vary during the simulation. Out behaves according to the expectations of a NAND gate. A latency t_{lat} must be considered for the information to reach the circuit output. (d) Information propagation results for the first input combination (ABC) = '000'. Pipelined information propagates along the circuit and a new input combination is fixed on the drivers.

the hexanethiol HT) to implement the NULL state. In this case, the cation characteristics are taken from literature [8]. It was obtained using the B3LYP functional and LANL2DZ basis set. The molecule was subjected to a static electric field parallel to the molecule principal axis. Fig.3(c) shows the bis-ferrocene VACT when an enhancing clocking field is applied to the molecule. The charge occupies DOT1 and DOT2, thus enabling information encoding in the two ferrocenes. Fig.3(d) shows the VACT evaluated for an inhibiting clocking field. When the clocking field is negative, the charge aggregates in the DOT3, suppressing the charge switch between the ferrocenes and permitting an effective NULL state. To demonstrate the exploitation and usefulness of the clocking system, we now simulate the 2-line molecular wire previously shown schematically in Fig.1(b). Three clock regions partition the device and are activated with synchronous clock signals, shown in Fig.3(e). The three clock regions are activated one after the other, whereas the two logic '0' and '1' sequentially propagate. Figure 3(f) demonstrates sequential activation of clocking regions. The data flows correctly along the wire, supported by the clocking system. Input changes are permitted once the first clock region enters the NULL state, demonstrating pipelined propagation without aberration.

In conclusion, this section demonstrates the importance of safely applying clock signals to propagate information along molFCN circuits. The clock applicability depends on the adopted molecule, which must present a third dot to host charges in the NULL state. Moreover, the findings show that we can simulate clocked molFCN at the circuit level by thoroughly analyzing the molecule physical and electrostatic properties.

G. The design of the 1-bit NAND

The analysis in Sec.III-F pointed out the bis-ferrocene molecule as a valid molecule solution for molFCN circuits and the need for a clocking mechanism to achieve pipelining. The mentioned considerations are at the basis of designing more complex digital gates and circuits, such as the 1-bit NAND presented in Fig.4(a). The NAND comprises an AND gate and an inverter (INV). The AND layout is the same as the MV, with input C fixed to logic '0' to obtain the gate behavior. The circuit is divided into four clock regions. The circuit area is 0.0004 μm^2. The clock signals controlling the regions are reported in Fig.4(b). Given the circuit complexity regarding the number of molecules and clock regions present, we used the flexibility of the MoSQuiTO simulation framework [12]. Specifically, the circuit design has been provided in MagCAD, which allows the graphical design of the circuit layout and clock region organization. Then, the circuit layout is exported into the SCERPA tool, translating the high-level design to evaluate the clocked information propagation [28]. The results of the SCERPA simulations are reported in Fig.4(c), which shows the values of the variable inputs A and B and the circuit output (Out). The circuit works according to the expectations, but a latency t_{lat} of approximately 2*T$_{ck}$ in providing the output must be considered, as Fig.4(c) shows. Therefore, the output information present in Fig.4(c) before t_{lat} cannot be considered valid since deriving from random charge configuration due to clock regions activation before actual input arrives. Moreover, Fig.4(d) reports the SCERPA step after t_{lat} when the information derived from (ABC) = '000' reaches the output. Contemporarily, the second input combination propagates along the AND output wire, and the third input combination (ABC) = '100' is fixed on the drivers. It is important to note that fabricating clock regions of the size presented is challenging, and here used for demonstrating modelling purpose only. Therefore, in the direction of pos-

sible prototypes, SAM-based circuits are being considered [29].

Overall, the adopted simulation framework efficiently performs circuit analysis. High-level circuit design can be performed with MagCAD, whereas the SCERPA algorithm solves the electrostatic interactions starting from single-molecule characterization. Therefore, the proposed framework is finally demonstrated to link the single-molecule physics to the high-level circuit design to provide feedback for future molFCN circuit evolution and prototyping.

IV. Conclusion

This work presents a comprehensive methodology for characterizing and modeling within the context of molFCN. By utilizing DFT for molecular analysis and integrating molecules into circuit simulation using SCERPA, we have demonstrated a systematic approach to understanding and designing molFCN circuits. Furthermore, this paper applies the methodology to the diallyl-butane cation, discussing the steps in molecule characterization and proposing circuit-level simulations. Simulation of a molecular wire has revealed critical design evaluation parameters, as the bistability factor, and emphasized the necessity of clocking systems in molFCN circuits. Therefore, we presented a 2-line molFCN wire and a NAND gate made by bis-ferrocene, which were analyzed using the same methodology. This demonstrates flexibility in designing circuits using different molecules.

Overall, this research contributes to realizing molFCN prototypes by offering a clear path for analyzing, designing, and implementing molFCN circuits. Future works will advance the characterization of complex logic gates, comprising timing considerations and fabrication feasibility assessments to compare molFCN with state-of-the-art technologies.

References

[1] C. S. Lent, B. Isaksen, and M. Lieberman, "Molecular quantum-dot cellular automata," *Journal of the American Chemical Society*, vol. 125, no. 4, pp. 1056–1063, 2003.

[2] Y. Wang and M. Lieberman, "Thermodynamic behavior of molecular-scale quantum-dot cellular automata (qca) wires and logic devices," *IEEE Transactions on Nanotechnology*, vol. 3, no. 3, pp. 368–376, 2004.

[3] Y. Ardesi, A. Gaeta, G. Beretta, G. Piccinini, and M. Graziano, "Ab initio molecular dynamics simulations of field-coupled nanocomputing molecules," *Journal of Integrated Circuits and Systems*, vol. 16, no. 1, pp. 1–8, 2021.

[4] F. Ravera, G. Beretta, Y. Ardesi, M. Krzywiecki, M. Graziano, and G. Piccinini, "A roadmap for molecular field-coupled nanocomputing actualization," in *2023 IEEE Nanotechnology Materials and Devices Conference (NMDC)*. IEEE, 2023, pp. 212–213.

[5] Y. Ardesi, G. Beretta, M. Vacca, G. Piccinini, and M. Graziano, "Impact of molecular electrostatics on field-coupled nanocomputing and quantum-dot cellular automata circuits," *Electronics*, vol. 11, no. 2, p. 276, 2022.

[6] Y. Ardesi, A. Pulimeno, M. Graziano, F. Riente, and G. Piccinini, "Effectiveness of molecules for quantum cellular automata as computing devices," *Journal of Low Power Electronics and Applications*, vol. 8, no. 3, 2018. [Online]. Available: http://www.mdpi.com/2079-9268/8/3/24

[7] V. Arima, M. Iurlo, L. Zoli, S. Kumar, M. Piacenza, F. Della Sala, F. Matino, G. Maruccio, R. Rinaldi, F. Paolucci *et al.*, "Toward quantum-dot cellular automata units: Thiolated-carbazole linked bis-ferrocenes," *Nanoscale*, vol. 4, no. 3, pp. 813–823, 2012.

[8] Y. Ardesi, G. Turvani, M. Graziano, and G. Piccinini, "Scerpa simulation of clocked molecular field-coupling nanocomputing," *IEEE Transactions on Very Large Scale Integration (VLSI) Systems*, vol. 29, no. 3, pp. 558–567, 2021.

[9] E. Blair and C. Lent, "Clock topologies for molecular quantum-dot cellular automata," *Journal of Low Power Electronics and Applications*, vol. 8, no. 3, p. 31, 2018.

[10] C. S. Lent and P. D. Tougaw, "Lines of interacting quantum-dot cells: A binary wire," *Journal of Applied Physics*, vol. 74, pp. 6227–6233, 1993. [Online]. Available: https://api.semanticscholar.org/CorpusID:4684392

[11] Y. Ardesi, L. Gnoli, M. Graziano, and G. Piccinini, "Bistable propagation of monostable molecules in molecular field-coupled nanocomputing," in *2019 15th Conference on Ph.D Research in Microelectronics and Electronics (PRIME)*, 2019, pp. 225–228.

[12] Y. Ardesi, U. Garlando, F. Riente, G. Beretta, G. Piccinini, and M. Graziano, "Taming molecular field-coupling for nanocomputing design," *ACM Journal on Emerging Technologies in Computing Systems*, vol. 19, no. 1, pp. 1–24, 2022.

[13] G. Beretta, Y. Ardesi, G. Piccinini, and M. Graziano, "Robustness of the in-plane data crossing for molecular field-coupled nanocomputing," in *2023 IEEE 23rd International Conference on Nanotechnology (NANO)*. IEEE, Jul. 2023.

[14] E. Rahimi and J. R. Reimers, "Molecular quantum cellular automata cell design trade-offs: latching vs. power dissipation," *Phys. Chem. Chem. Phys.*, vol. 20, no. 26, pp. 17 881–17 888, 2018.

[15] K. Walus, T. J. Dysart, G. A. Jullien, and R. A. Budiman, "Qcadesigner: a rapid design and simulation tool for quantum-dot cellular automata," *IEEE Transactions on Nanotechnology*, vol. 3, no. 1, pp. 26–31, March 2004.

[16] F. Riente, U. Garlando, G. Turvani, M. Vacca, M. R. Roch, and M. Graziano, "Magcad: A tool for the design of 3d magnetic circuits," *IEEE Journal on Exploratory Solid-State Computational Devices and Circuits*, vol. 3, pp. 65–73, 2017.

[17] U. Garlando, M. Walter, R. Wille, F. Riente, F. S. Torres, and R. Drechsler, "Topolinano and fiction: Design tools for field-coupled nanocomputing," in *2020 23rd Euromicro Conference on Digital System Design (DSD)*. IEEE, 2020, pp. 408–415.

[18] A. S. Bonilla, R. Gutierrez, L. M. Sandonas, D. Nozaki, A. P. Bramanti, and G. Cuniberti, "Structural distortions in molecular-based quantum cellular automata: a minimal model based study," *Physical Chemistry Chemical Physics*, vol. 16, no. 33, pp. 17 777–17 785, 2014.

[19] M. D. Hanwell, D. E. Curtis, D. C. Lonie, T. Vandermeersch, E. Zurek, and G. R. Hutchison, "Avogadro: an advanced semantic chemical editor, visualization, and analysis platform," *Journal of cheminformatics*, vol. 4, pp. 1–17, 2012.

[20] F. Neese, "The orca program system," *Wiley Interdisciplinary Reviews: Computational Molecular Science*, vol. 2, no. 1, pp. 73–78, 2012.

[21] ——, "Software update: the orca program system, version 4.0," *Wiley Interdisciplinary Reviews: Computational Molecular Science*, vol. 8, no. 1, p. e1327, 2018.

[22] G. Beretta, Y. Ardesi, G. Piccinini, and M. Graziano, "vlsi-nanocomputing/scerpa: Scerpa v4.0.1," Dec. 2022. [Online]. Available: https://doi.org/10.5281/zenodo.7457038

[23] F. Weigend and R. Ahlrichs, "Balanced basis sets of split valence, triple zeta valence and quadruple zeta valence quality for h to rn: Design and assessment of accuracy," *Physical Chemistry Chemical Physics*, vol. 7, no. 18, p. 3297, 2005.

[24] Y. Ardesi, M. Graziano, and G. Piccinini, "A model for the evaluation of monostable molecule signal energy in molecular Field-Coupled nanocomputing," *J. Low Power Electron. Appl.*, vol. 12, no. 1, p. 13, Mar. 2022.

[25] S. Grimme, J. Antony, S. Ehrlich, and H. Krieg, "A consistent and accurate ab initio parametrization of density functional dispersion correction (dft-d) for the 94 elements h-pu," *The Journal of Chemical Physics*, vol. 132, no. 15, p. 154104, 2010.

[26] S. Grimme, S. Ehrlich, and L. Goerigk, "Effect of the damping function in dispersion corrected density functional theory," *Journal of Computational Chemistry*, vol. 32, no. 7, pp. 1456–1465, 2011.

[27] U. C. Singh and P. A. Kollman, "An approach to computing electrostatic charges for molecules," *Journal of Computational Chemistry*, vol. 5, no. 2, pp. 129–145, 1984.

[28] Y. Ardesi, G. Turvani, M. Graziano, and G. Piccinini, "Scerpa simulation of clocked molecular field-coupling nanocomputing," *IEEE Transactions on very large scale integration (VLSI) systems*, vol. 29, no. 3, pp. 558–567, 2021.

[29] Y. Ardesi, G. Beretta, C. Fabiano, M. Graziano, and G. Piccinini, "A reconfigurable field-coupled nanocomputing paradigm on uniform molecular monolayers," in *2021 International Conference on Rebooting Computing (ICRC)*. IEEE, 2021, pp. 124–128.